

F-TEST IN MATCHED FIELD PROCESSING: IDENTIFYING MULTIMODE PROPAGATION

C.F. Mecklenbräuer¹, D. Maiwald², J.F. Böhme¹

¹ Dept. of Electrical Engineering, Ruhr University Bochum, D-4470 Germany

email: cfm@sth.ruhr-uni-bochum.de

² FGAN/FFM, Wachtberg-Werthhoven, D-53343 Germany

ABSTRACT

In this paper, we address the simultaneous detection and classification of signal arrivals, as well as the estimation of source parameters of signals impinging on an array of sensors. We develop a procedure for short-time stationary broadband signal propagation in a shallow ocean. The procedure will be applied to sensor data obtained from a towed horizontal receiver array in the Baltic Sea for interpreting the impinging signals.

We apply a multiple test procedure to three propagation models: a Green's function model, uncorrelated normal modes and plane waves. We apply an *F*-test which calculates signal to noise ratios for the three models, and select the model with highest SNR. Thereby, we are able to classify previous phantom bearing estimations as uncorrelated normal mode propagation originating from the towing ship itself.

1. INTRODUCTION

We investigate an algorithm for testing how many signals are impinging on the array in a specified time interval. This method has been successfully applied to seismic data [1] and sonar data [2] in the context of plane wave models before. In this contribution we apply the combined estimation- and test-procedure in a matched-field approach to data obtained by a towed horizontal array. The steering vector is replaced by a model vector which contains samples of the Green's function to the acoustic propagation problem. In this way, we incorporate effects of correlated signal arrivals directly into the model.

To be able to identify signal arrivals which originate from the same source, but have lost their cross-correlation underway between source and receiver, we develop a model with uncorrelated normal modes.

Furthermore, we are able to identify the impinging signals as stemming from one of three selected models. We calculate the broadband *F*-variable for the three models presented in sec. 2 and selected the maximum

value among them.

The paper is organized as follows: in the next section we formulate the acoustic propagation model. Section 3 is devoted to the data model. In sec.4 we briefly describe the theoretical background of the *F*-test applied to our propagation models. Thereafter, we present some experiments conducted with real world passive sonar data. We conclude with some remarks.

2. PROPAGATION MODELS

The Green's Function $G(\underline{r}, \underline{r}_o, \omega)$ is the acoustic response observed at location $\underline{r} = (r, \varphi, z)$ to a monochromatic point source at $\underline{r}_o = (r_o, \varphi_o, z_o)$. The solution to the wave equation for a horizontally stratified ocean is expanded in a discrete set of normal modes ψ_α ($\alpha = 1 \dots A$), which is an accurate approximation if the signal source is located not too closely to the receiving array

$$G(\underline{r}, \underline{r}_o, \omega) = \sum_{\alpha=1}^A \psi_\alpha(z) \psi_\alpha(z_o) H_0^{(1)}(k_\alpha R). \quad (1)$$

More precisely, we neglect the contribution of the continuous eigen values of the associated Sturm-Liouville equation. $H_0^{(1)}$ denotes the Hankel function. R is the horizontal distance between source- and observation point. The modal functions ψ_α and corresponding wave-numbers k_α are obtained numerically by solving a Sturm-Liouville eigenvalue problem subject to a Dirichlet boundary condition at the ocean surface and the Sommerfeld radiation condition in the sub-bottom region [3]. For the *F*-Test described in section 4 we use the following three signal propagation models.

(M1) Green's function model with correlated normal modes: the Green's function (1) is sampled at N sensor locations, which are stacked into the steering vector \underline{g} . (M2) An incoherent normal mode model. The individual modes have lost their cross-correlation properties during their individual travel from source to receiver. For that we introduce uncorrelated random factors of the terms summed up in (1).

For this model, we use as much steering vectors $\underline{\psi}$ per source as there are modes arriving from.

(M3) For far field sources we used propagation in form of plane waves $e^{jkr \cos \beta}$.

3. DATA MODEL

We use the propagation model to describe the output of the horizontal sensor array with N elements. The array output is sampled after low pass filtering and divided into K stretches of duration T . Each of these data stretches in turn are divided into K' time pieces of length $T' = T/K'$. They are short time Fourier-transformed using multiple windows [4] to obtain $\underline{X}_{k,l}(\omega)$ for $k = 1 \dots K'$ and $l = 0, \dots, (L-1)$. The number L of orthonormal windows used depends on the selected analysis bandwidth W . Here, we used $W = 1 \text{ Hz}$.

$$\underline{X}_{k,l}(\omega) = \sum_{t=0}^{T'-1} \nu_t^{(l)}(T, W) \underline{x}(t + T'k) e^{-j\omega t}, \quad (2)$$

with a set of orthonormal data tapers $\nu_t^{(l)}(T, W)$ (the Slepian sequences, see [5]).

The cross spectral density matrix (CSDM) of the sensor data $\underline{C}_X(\omega)$ is estimated non-parametrically by

$$\hat{\underline{C}}_X(\omega) = \frac{1}{K'} \sum_{l=0}^{L-1} \sum_{k=1}^{K'} \underline{X}_{k,l}(\omega) \underline{X}_{k,l}^*(\omega) \quad (3)$$

during each time-step. This is motivated by the asymptotic independence of Fourier-transformed stretches and the orthogonality of the Slepian windows.

The CSDM of the array output can be expressed by $\underline{C}_X(\omega, \underline{\vartheta}_\omega) = \underline{H}(\omega, \underline{\xi}) \underline{C}_S(\omega, \underline{\vartheta}_\omega) \underline{H}^*(\omega, \underline{\xi}) + \nu(\omega) \underline{I}$ where \underline{C}_S is the diagonal CSDM of the signals and $\nu(\omega)$ is the CSDM of sensor noise¹. Diagonality of the noise term $\nu(\omega) \underline{I}$ is justified by choosing sensor spacing larger than the correlation length of environmental noise.

Vector $\underline{\vartheta}_\omega$ summarizes all unknown parameters at ω . These parameters can be divided into those, that enter linearly into the model, i.e. $\nu(\omega)$ and the vector $\underline{\vartheta}_\omega^*$, and those parameters $\underline{\xi}$ that enter in a nonlinear fashion (source positions, etc). The columns of the transfer function $\underline{H}(\omega, \underline{\xi})$ consist of a combination of the model vectors $\underline{g}, \underline{d}, \underline{\psi}$

$$\underline{H}(\omega, \underline{\xi}_M) = (\dots \underline{g} \dots \underline{d} \dots \underline{\psi} \dots)$$

and depends on the unknown locations \underline{r}_{om} of $m = 1 \dots M$ sources which are summarised in a single parameter vector $\underline{\xi}_M$.

The distribution of $\underline{X}_{k,l}(\omega)$ is known asymptotically: they are approximately independent and identically complex normal random vectors, with zero mean and CSDM $\underline{C}_X(\omega, \underline{\vartheta}_\omega)$. Approximate conditional ML estimates for the broadband case based on these assumptions are described previously [6].

¹the asterisk * means conjugate transpose

4. MATCHED FIELD F-TEST

The transformed data (2) are known to be asymptotically conditionally normal distributed with mean $\underline{H}(\omega, \underline{\xi}) S_{k,l}(\omega)$ and covariance matrix $\nu \underline{I}$. The Fourier-transformed signal $S_{k,l}(\omega)$ is defined similar to (2). This motivates the application of a sequential F -test for simultaneous signal detection, classification and source parameter estimation. The theoretical background for the F -Test in the single frequency case can be found in Shumway [7]. The broadband case is described e.g. in [1, 2] for plane waves in sonar and seismic context.

The F -test constructs ratios of estimated signal- and noise power quantities. In the numerical procedure we do not use the data (2) directly, instead we reformulate the underlying equations, such that the measurement data enter the procedure solely by the estimated CSDM (3).

Information about the assumed signal propagation model (i.e. the environmental parameters, which are contained in the Green's function) enters by means of projection matrices, operating on the estimated CSDM.

Suppose, we have already detected M signals, and have estimated their associated positional and spectral parameters. We construct the two projection matrices $\underline{P}_M = \underline{P}(\omega, \underline{\xi}_M)$ and $\underline{P}_{M+1} = \underline{P}(\omega, \underline{\xi}_{M+1})$, which project onto the signal subspaces of the first M and $M+1$ signals, respectively. Generally, for large T , the statistic of the ratio of the sum of squared residuals (SSR) and the sum squared errors (SSE)

$$F_{M+1}(\omega, \underline{\xi}_{M+1}) = \left(\frac{\nu_2}{\nu_1} \right) \frac{\text{tr} \left[(\underline{P}_{M+1} - \underline{P}_M) \hat{\underline{C}}_X \right]}{\text{tr} \left[(\underline{I} - \underline{P}_{M+1}) \hat{\underline{C}}_X \right]} \quad (4)$$

is doubly non-central F -distributed. However, if there is no signal present, it can be approximated by a central F -distribution² with $\nu_1 = K'(2 + p_{\underline{\xi}_{M+1}})$ and $\nu_2 = K'(2N - 2(M+1) - p_{\underline{\xi}_{M+1}})$ degrees of freedom [7]. For $\omega_i \neq \omega_j$ the random variables $F_{M+1}(\omega_i, \underline{\xi}_{M+1})$, $F_{M+1}(\omega_j, \underline{\xi}_{M+1})$ are asymptotically i.i.d. with mean 1 and variance $\frac{2\nu_2^2(\nu_1 + \nu_2 - 2)}{\nu_1(\nu_2 - 2)^2(\nu_2 - 4)}$. Finally, we arrive at the broadband statistic

$$F_{M+1}(\underline{\xi}_{M+1}) = \frac{1}{L} \sum_{i=1}^L F_{M+1}(\omega_i, \underline{\xi}_{M+1}), \quad (5)$$

The exact distributional properties of this quantity are not known to the authors. One way of approaching this problem is by approximating $F_{M+1}(\omega_i, \underline{\xi}_{M+1})$ by

²the dimension of vector $\underline{\xi}$ describing the nonlinear parameters of a wave is denoted by $p_{\underline{\xi}}$.

a $\chi^2_{\nu_1}$ distributed random variable. If ν_2 is large, then $\frac{1}{\nu_1 L} F_{M+1}(\xi_{M+1})$ is $\chi^2_{(\nu_1 L)}$ -distributed.

The procedure is initialised with the null projector $P_0(\omega) \equiv 0$. Each test stage in this multiple test procedure is preceded by the estimation of the parameters of an additional source by maximizing (5) or equivalently solving the equation of the conditional maximum likelihood estimator (CMLE). If the maximum exceeds the threshold, a new source is detected and the parameters of all detected sources are simultaneously corrected by further maximizing (5).

For the experiments described below, we used a mixed model of near-field coherent and incoherent multimode propagation for some sources and a plane wave model for sources in large distance from the receiver array.

5. EXPERIMENTS AND CONCLUSION

The sensor data is recorded in the Baltic Sea (Ocean depth $\approx 50m$) with a towed line array of $N = 15$ sensors equi-spaced by 2.56 m. Sampling frequency was $f_s = 1024 Hz$ after low pass filtering with cut off $f_c = 256 Hz$. We use a sequence of 10 minutes, divided into $K = 150$ stretches of $T = 4s$ each, in which a scenario of four broadband sources is present. In (3) we averaged over $K' = 16$ periodograms. Analysis bandwidth in (2) was $W = 1 Hz$. The figures below show some of the obtained results.

Figure 1 shows the result of an F -test with plane wave model (M3) for all sources. We can clearly observe 5 plane waves impinging on the array. During the experiment only 4 ships were present: the ships associated with the initial bearings at $82^\circ, 105^\circ, 150^\circ$ and the towing ship at endfire-position 0° . The bearings at $22^\circ, 40^\circ$ are phantoms.

Secondly, we applied an F -test for model (M1) for all sources. This approach didn't work well. We will clarify the reason below. Next, we used the following subtractive method: The co-ordinates of the towing ship are estimated for each data stretch individually by the method presented in [3]. We subtract the associated multimode signal from the data in frequency domain and apply the presented matched-field F -test with a mixed multimode and plane wave model (M3). The source at bearing 150° is modeled by plane waves, whereas all other sources are modeled by the Green's function approach (M1). The result is presented in fig.2. Unexplained bearing estimations which do not correspond to any ships in the given scenario, at bearings 22° and 40° [2] vanish in this figure. Thereby we had stronger reason to believe that the signals at these bearings indeed belong to multimode signals emitted by the towing ship itself.

Further evidence was supported by simulations carried out by T.Purkop [8], where a single broadband source with the same spectral density as our real data and model (M1) was swepted from 0° to 180° around the sensor array, see fig. 3. For the source location at end-fire position $\varphi_0 = 0^\circ$ the F -Test with model (M3) showed up the estimations at $22^\circ, 40^\circ$.

Finally, we applied the following approach for simultaneous detection, classification and parameter estimation: We calculated the F -variable for all three models (M1–3) and selected the absolute maximum among them. If this value is higher than a certain threshold, we decide in favour of having a signal impinging on the array. This procedure classifies a signal as one of the three models. The results are shown in fig.4.

We have shown that an F -test can be used as a flexible signal processing tool, capable of signal detection, classification of sources and estimating their parameters.

ACKNOWLEDGEMENTS

We thank S.Brandhoff for implementing parts of the signal processing and thank Atlas Elektronik/Bremen for providing the data. We are indebted to M.Blaha for correcting the manuscript.

6. REFERENCES

- [1] D. Maiwald and J.F. Böhme, "Multiple testing for seismic data using bootstrap", in *Proc. IEEE Int. Conf. Acoust., Speech, Signal Processing*, Adelaide, 1994.
- [2] J.F. Böhme and D. Maiwald, "Multiple wideband signal detection and tracking from towed array data", in *SYSID 94, 10th IFAC Symposium on System Identification*, M. Blanke and T. Söderström, Eds., Copenhagen, July 4-6 1994, vol. 1, pp. 107–112, Danish Automation Soc.
- [3] C.F. Mecklenbräuker and J.F. Böhme, "Matched field processing in shallow ocean: Identification of multimode propagation", in *Second European Conference on Underwater Acoustics*, Copenhagen, July 4-8 1994, European Commission, pp. 611–616.
- [4] D.J. Thomson, "Jackknifing multiple-window spectra", in *Proc. IEEE ICASSP*, Adelaide, April 19-22 1994, IEEE, pp. VI-73 – VI-76.
- [5] D. Slepian, "Prolate spheroidal wave functions, fourier analysis, and uncertainty- v: The discrete case", *Bell System Tech. J.*, vol. 57, pp. 1371–1429, 1978.
- [6] J.F. Böhme, "Array processing", in *Advances in Spectrum Analysis and Array Processing*, S. Haykin, Ed., pp. 1–63. Prentice Hall, Englewood Cliffs N.J., 1991.
- [7] R.H. Shumway, "Replicated time-series regression: An approach to signal estimation and detection", in *Handbook of Statistics, Vol. 3*, D.R. Brillinger and P.R. Krishnaiah, Eds., pp. 383–408. Elsevier Science Publishers B.V., 1983.
- [8] T. Purkop, "Anwendung des F-Tests auf Sonardaten im Flachwasser: Ebene Wellen und Modenausbreitung", Studienarbeit, Ruhr-Universität Bochum, Bochum, Germany, 1994.

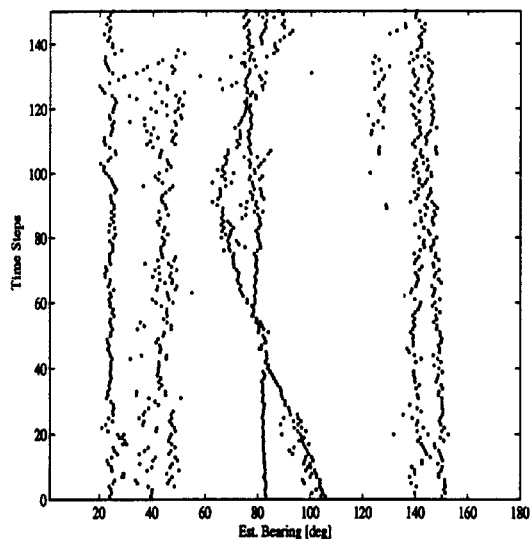


Figure 1: *F*-Test for plane wave model applied to real sonar data. The left two traces at 22° and 40° could not be identified with source locations

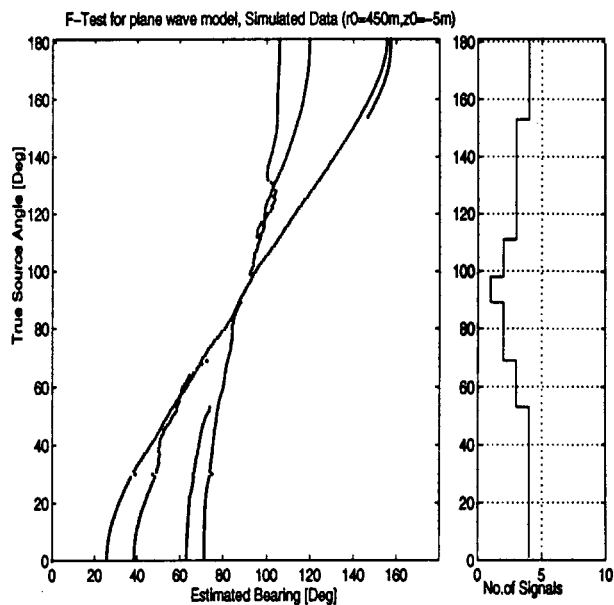


Figure 3: *F*-Test for plane wave model applied to simulated data from *Green's function model* with source located at distance $r_0 = 450m$, depth $z_0 = -5m$ and cylinder co-ordinate angle φ_0 was swept from 0° to 180°.

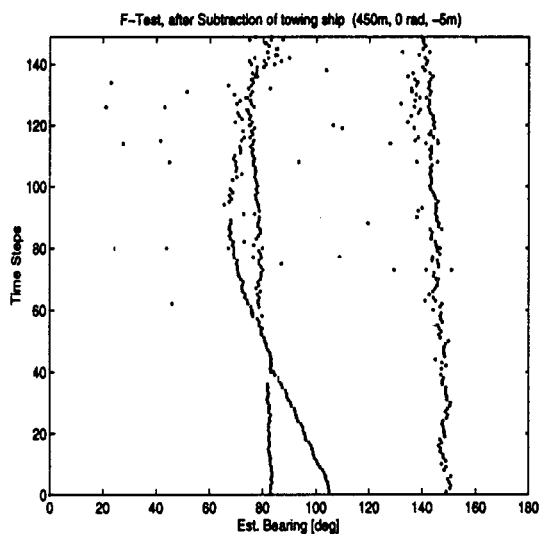


Figure 2: Results of the *F*-Test with *Green's function model* applied to real data after subtracting the signal of the towing ship

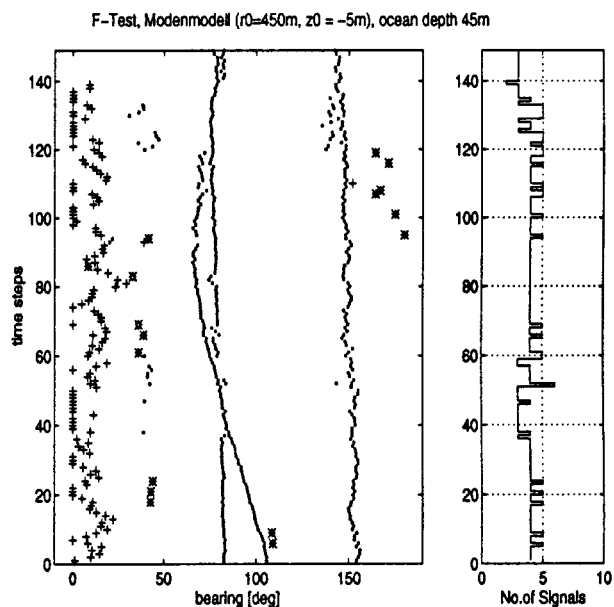


Figure 4: Mixed model *F*-Test with the following three models described in sec.2, +:uncorrelated normal-mode, *:Green's function, •:plane waves. The figure shows the estimated bearings and the signal classifications.